Real-time monitoring system of composite aircraft wings utilizing Fibre Bragg Grating sensor

You may also be interested in:

Alternate Data Acquisition and Real-time Monitoring System on HT-7 Tokamak
Wei Peijie, Luo Jiarong, Wang Hua et al.

Real-Time Monitoring System of Pulse Durations of Picosecond Ti:Sapphire Laser
Motonobu Sasaki, Shujie Lin, Motowo Tsukakoshi et al.

Monitoring Conditions of Cantilever during Conducting Atomic Force Microscopy Spectroscopy
Measurements
Tsunehiro Oohira and Atsushi Ando

Monitoring System for Slope Stability under Rainfall by using MEMS Acceleration Sensor IC tags
S Murakami, A Dairaku, H Komine et al.

A Real-time Monitoring System for the Pipeline Network of Coalmine
H L Zhao, J K Wang and X Jiang

A Real-Time Monitoring System Using a Multimodal Sensor with an Electrical Conductivity Sensor and
a Temperature Sensor for Cow Health Control
Masato Futagawa, Taichi Iwasaki, Mitsuyoshi Ishida et al.

Real-time monitoring system of composite aircraft wings utilizing Fibre Bragg Grating sensor

E Vorathin[1*], Z M Hafizi[1], S A Che Ghani[2] and K S Lim[3]

[1]Advanced Structural Integrity and Vibration Research (ASIVR), Faculty of Mechanical Engineering, Universiti Malaysia Pahang, Malaysia
[2]Human Engineering Group (HEG), Faculty of Mechanical Engineering, Universiti Malaysia Pahang, Malaysia
[3]Photonics Research Centre, Faculty of Science, Universiti Malaya, Malaysia

*vora.91.11@hotmail.com

Abstract. Embedment of Fibre Bragg Grating (FBG) sensor in composite aircraft wings leads to the advancement of structural condition monitoring. The monitored aircraft wings have the capability to give real-time response under critical loading circumstances. The main objective of this paper is to develop a real-time FBG monitoring system for composite aircraft wings to view real-time changes when the structure undergoes some static loadings and dynamic impact. The implementation of matched edge filter FBG interrogation system to convert wavelength variations to strain readings shows that the structure is able to response instantly in real-time when undergoing few loadings and dynamic impact. This smart monitoring system is capable of updating the changes instantly in real-time and shows the weight induced on the composite aircraft wings instantly without any error. It also has a good agreement with acoustic emission (AE) sensor in the dynamic test.

1. Introduction

Studies over the last decades have shown great interest in the use of composite structures such as fibre reinforce polymer (FRP) in engineering applications due to their high strength-to-weight ratio [1, 2]. Aerospace engineering is one of the major and critical engineering applications that implement the use of composite structures. According to [3], deployment of composite structures in Boeing 787 aircraft has increased by 38 percent compared to Boeing 777 aircraft, which utilizes 12 percent of composite structures in its manufacturing. Materials used in manufacturing the Boeing 787 aircraft are shown in Figure 1. Aircraft wings and fuselage employ the most composite materials and they are always the critical areas that prone to deformation and damage. Due to the layer by layer lamination, composite structures are prone to unforeseen damage such as cracks and delamination [4-6] after a certain period of performance. The damage must be monitored prior to further enormous deformation that can affect performance or the cause of catastrophic, which is the sudden damage of the structure.

The monitoring of a structural health condition is known as structural health monitoring (SHM). SHM is a process that involves the observation of dynamic response from an arrangement of sensors periodically over time [2]. The implementation of SHM in composites will lead to the development of smart structure in which the structure can give real time stimulation according to the environmental changes that it experienced. The topic of smart structure is relatively new and is commencing to be

qualified as a distinct field of applied since in 1980 [7]. The smart structure can have distinct ways of analysis method where it can be examined as a whole structure or only focused on a specific part of it, which is a single structural element [8].
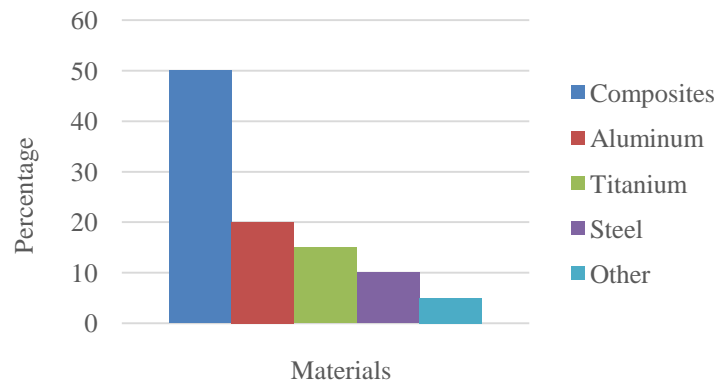

Figure 1. Materials utilization in Boeing 787 manufacturing

Aircraft wings experienced the most deflection during take-off, in which this phenomenon must be monitored before severe damage happened to the wings. Several studies [2, 3, 9-12] have been carried out with the embedment of Fibre Bragg Grating (FBG) sensors in the aircraft's composite structures, especially wings, and it is acknowledged that properties such as small diameter, multiplexing ability and immunity to electromagnetic fields [13-16] are the primary attractive characteristics of FBGs in replacing conventional sensors like piezoelectric and strain gauge for SHM in composites. However, the search for a robust and interactive real-time monitoring system that can alert the end user instantly is still far behind in achieving the idealized concept of smart structure. This drawback has caught the intention of the authors in developing a robust real-time monitoring system to monitor the deflection of the aircraft wings. At the end of this study, for a proof of concept, a fiberglass plate lamination to represent the aircraft wing was fabricated. The FBG instrumentation system and real-time MATLAB processing software are illustrated when the structure undergoes several static loads experimentation.

2. Fibre Bragg Grating (FBG) sensor instrumentation and working principle
The use of FBGs in composites has shown great interest during the late 20[th]century [17]. FBGs sensing principle enquires light source to sense the physical phenomenon.The basic working principle of FBG is by reflecting a specific wavelength of the emitted light source depending on the Bragg properties [18] as shown in Figure 2.
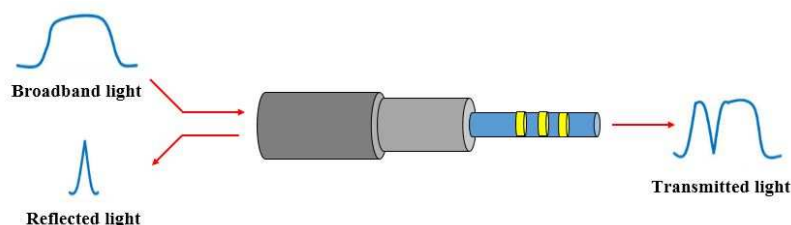

Figure 2. The working principle of FBG sensor

As the optical fibre is in tension, the gap of the Bragg gratings will be wider and vice versa when the optical fibre is in compression. The advantages of FBG as compared to the electrical sensor are shown in Table 1 [19]. The gratings area of FBG is a laser-inscribed region, which reflects the narrow band light corresponding to the Bragg wavelength, λ_B (as calculated by Equation 1) [20] where Λ is the grating period and n is the refractive index of the grating.

$$\lambda_B = 2n\Lambda \qquad (1)$$

The refractive index of the grating is fixed when the FBG experienced strain, which results in the linearity between the grating period and strain. Therefore, any change in the measurement will result in the shift of the reflected wavelength. The wavelength will shift to the positive region when expanding and vice versa when contracting. The relative change in the wavelength are given as Equation 2 [21], where C_s is the coefficient of strain ε, C_T is the coefficient of temperature and ΔT is the change in the temperature.

$$\frac{\Delta \lambda_B}{\lambda_B} = C_s \varepsilon + C_T \Delta T \tag{2}$$

Table 1. Comparison between optical fibre sensor and an electrical sensor

Media	Technology	Electrical noise immunity	Measurement speed	Sensor Configuration	Mounting
Electrical	Foil gauges	Low	~ 100 kHz	Single point	Surface mount
	Vibrating wire	Moderate	~ 1 kHz	Single point	Embeddable
Optical	Fibrebragg grating	Complete	< 1 kHz	Multi sensor	Surface mount and embeddable

In order for FBG to function, an interrogation system, which is the signal transmitter and receiver, is needed. Matched edge filter detection interrogation system is the simplest and cheapest in cost as compared to other interrogation system [22]. The configuration of the matched edge filter interrogation system is shown in Figure 3 below.
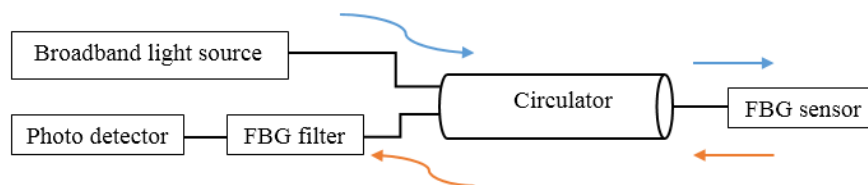

Figure 3. Matched edge filter system configuration

The system is started off with broadband light source emitted light across the optical circulator and into the FBG sensor. Gratings on the FBG will reflect the light back to the optical circular, which is functioning to circulate and convey the light passes through the FBG filter and into the photo detector. The photo detector or Photodiode (PD) functions to convert the light source into an electrical signal to be processed by the expert. The shaded area is the light intensity identified by the photo detector when the FBG sensor undergoes tension or compression [22].

3. Experimentation

3.1. Sample fabrication
A ten-layer woven fibreglass composite plate with hand lay-up lamination was fabricated to represent the aircraft wing structure. The dimension of the composite plate is 40 cm x 40 cm x 0.8 cm and it was cured with the use of glycidyl (GL) epoxy and hardener as resin. A single 1550 nm FBG sensor was positioned in the middle of the ninth and tenth layer of the composite plate. Figure 4(a) shows the woven fibreglass used and Figure 4(b) shows the cured composite plate with embedded FBG sensor.
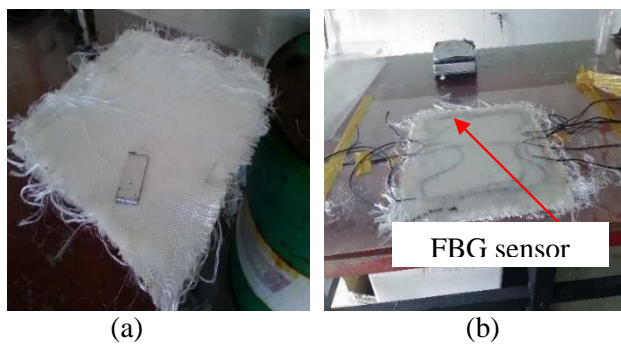
Figure 4. Fabrication process (a) Woven fibreglass, (b) Embedded FBG sensor
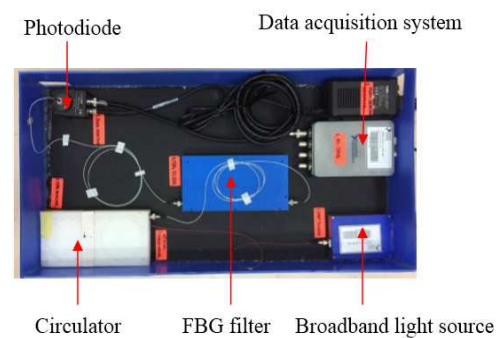

Figure 5. Matched edge filter interrogation configuration

3.2. Experimental set-up

Matched edge filter interrogation system, as shown in Figure 5, was set up for the experimentation. Broadband light source of power 20mW and 99.9% reflectivity of both FBG sensor and filter, and 3-port optical circular was used in the interrogation system. PDA10CS-EC photodiode manufactured by THORLABS was used for the conversion of light wavelength to an electrical voltage signal. NI 9234 data acquisition system from NATIONAL INSTRUMENTS was connected to PD for data acquisition. Figure 6 shows the set-up of the experimentation.

3.3. Experimental procedure

For the static loading test, a weight support stand as shown in Figure 6(a) was placed on top of the composite plate so that the distribution of loads is equal and the same at all time. 10 N and 20 N of loads as in Figure 6(b) were applied on the composite plate. The composite plate was first subjected to 10 N load, and the voltage reading and weight measurement reading were recorded and the condition of the composite plate was observed. The experiment was repeated for a load of 20 N, 30 N, 40 N and 50 N. MATLAB software was used to create graphical user interface (GUI) as virtual instrumentation tool to display the real-time deflection of the composite plate as it undergoes static point loading. Mesh grid of -10 to 10 in x- and y- axis, and 0 to 100 in z-axis artificial sample elements with four fixed locations was programmed and the prediction of strain distribution was based on the voltage reading from the FBG.
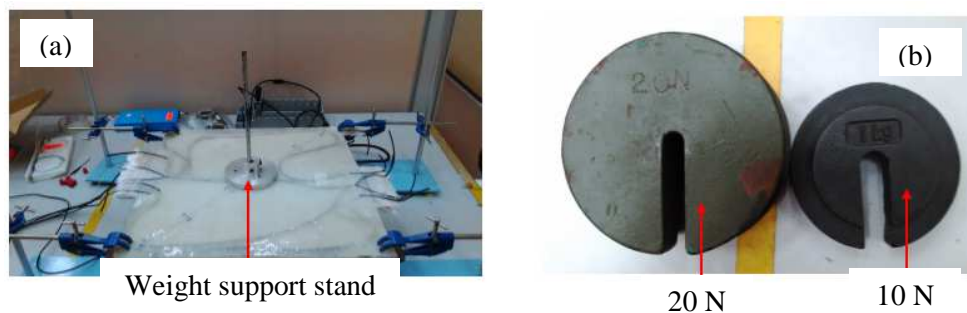

Figure 6. Experimental set-up: (a) Weight support stand, (b) Loads

For the dynamic impact test, an AE sensor was attached to the surface of the composite plate at the same position as the FBG sensor as shown in Figure 7. Three times of impact were induced with an impact hammer at a distance of 15 cm away from both the sensors' placement. The composite plate was clamped at four side corners for a better performance and away from surrounding perturbation.

MATLAB GUI with sampling rates of 1000 Hz for both FBG and AE sensors was programmed to capture the raw impact signal simultaneously. These raw signals were then transformed using Fast Fourier Transform (FFT) to the frequency domain and acquitted at frequency length of 500 Hz. The real-time natural frequency from both sensors was then captured simultaneously and compared with theoretical prediction using ABAQUS.

In Abaqus' FEA analysis, four points of the plate were fixed as the boundary conditions and the maximum frequency to be obtained was set at 500 Hz. Figure 8(a) shows the four fixed points as the boundary conditions of the composite plate and Figure 8(b) shows the meshed composite plate. Table 2 tabulates the mechanical properties of the material [23].
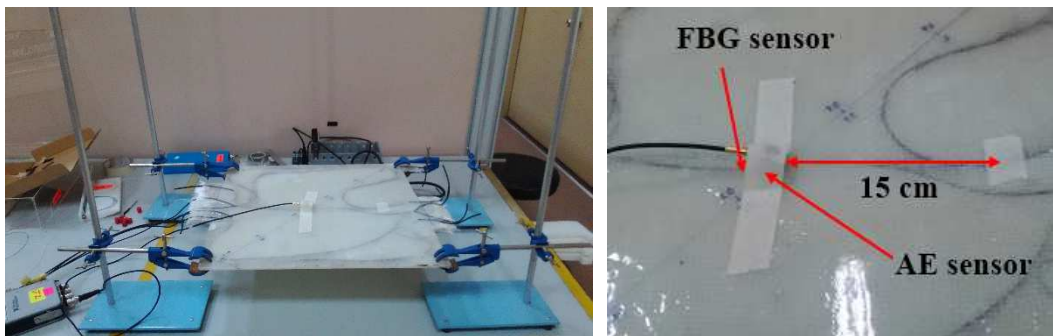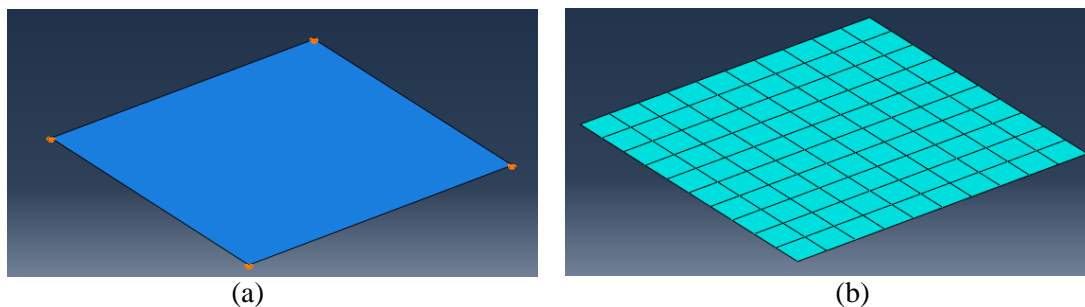

Figure 7. Dynamic impact test experimental setup

(a)   (b)

Figure 8. Abaqus analysis: (a) Fixed points of the boundary conditions, (b) Meshed composite plate

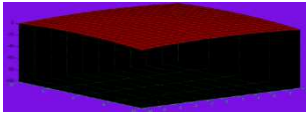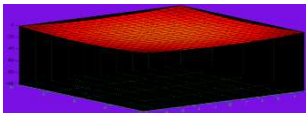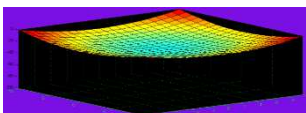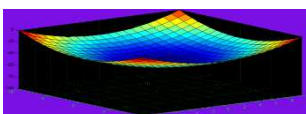**Table 2.** Mechanical properties of the material
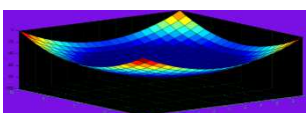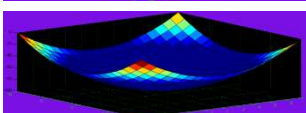
$E_{xx} = E_{yy}$ [Mpa]	E_{zz}[Mpa]	$V_{yx} = V_{xy}$	$V_{yz} = V_{xz}$	G_{xy} [Mpa]	$G_{yz} = G_{zx}$ [Mpa]	ρ [kg/m^3]
60500	62356	0.075	0.4693	3900	1700	1100

4. Results and discussion

Table 3 shows the summarization of the static loading results. From the results of the experimentation, the composite plate condition shows that it is in a flat condition that implies it does not experience any strain when no load is applied. This condition can be verified from the weight measured reading where it showed 0 N. The structure condition started to deflect slightly when the 10 N load was applied to the composite.

Deflection of the composite plate sank slightly bigger and the voltage increased to 3.7 V when the load was increased to 20 N. The colour at the middle of the composite plate condition turned blue to indicate that strain experienced the most at the middle part. The maximum that can be measured by the thin composite plate is 50 N with a voltage of 4 V. The composite plate detects the load applied without any error. Linearity between the increase of weight and voltage are shown in Figure 9. The conversion of voltage to Newton was by calibration with the substitution of linearity equation obtained from the linearity graph in Figure 9.

Table 3. Summary of static loadings results

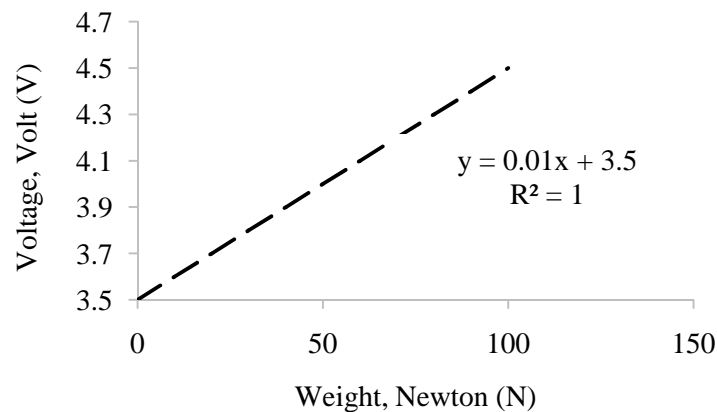| Load (N)	Structure condition	Voltage (V)	Weight measured(N)
0		3.5	0
10		3.6	10
20		3.7	20
30		3.8	30
40		3.9	40
50		4.0	50

$$y = 0.01x + 3.5$$
$$R^2 = 1$$

Figure 9. Voltage vs weight linearity graph

Figure 10 shows the impact seismic raw signal of FBG and AE sensor while Figure 11 shows one out of three trials comparison between FBG and AE sensor natural frequency signal. Table 4 tabulates the summarization of natural frequency results from both sensors while Table 5 shows the comparison of average natural frequency from both the sensors with theoretical Abaqus analysis.

ABAQUS FEA has predicted 4 modes of vibration for frequency below 500 Hz. Mode shape 1 (99.5 Hz) and mode shape 4 (373.81 Hz) indicate the dominance of flexural wave propagation. These wave propagation phenomena can be further verified from the high amplitude of natural frequency picked up by both the FBG (89.2 Hz, 401.3 Hz) and AE (91.2 Hz, 402 Hz) sensors. Both sensors are sensitive to flexural type wave propagation in which this type of wave induced a natural axial strain on the sensors. The FBG sensor also capable to captured slight twisting mode of wave propagation, which are mode 2 and mode 3, with a similar predicted natural frequency value of 181.02 Hz. However, the

amplitude was relatively small compared to flexural mode wave propagation. This signifies that the embedded FBG sensor is capable to capture all the important natural frequencies of various mode wave propagation. In Figure 11, the natural frequency sharp peak stood out from the rest of the noise signal.
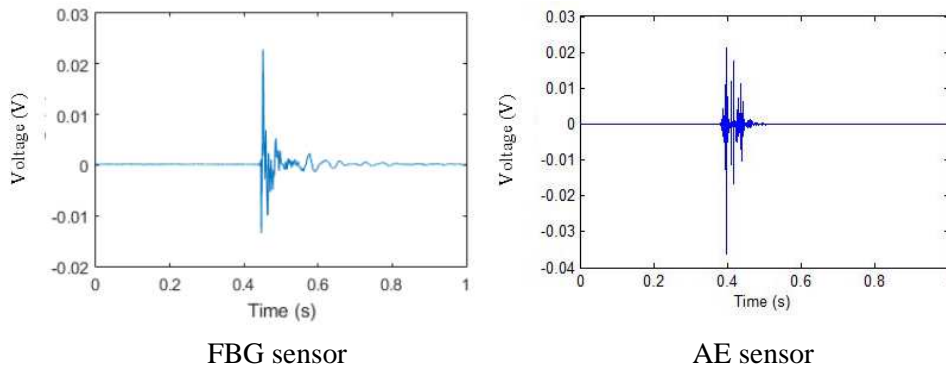

FBG sensor   AE sensor

Figure 10. Comparison of impact signal between FBG and AE sensor

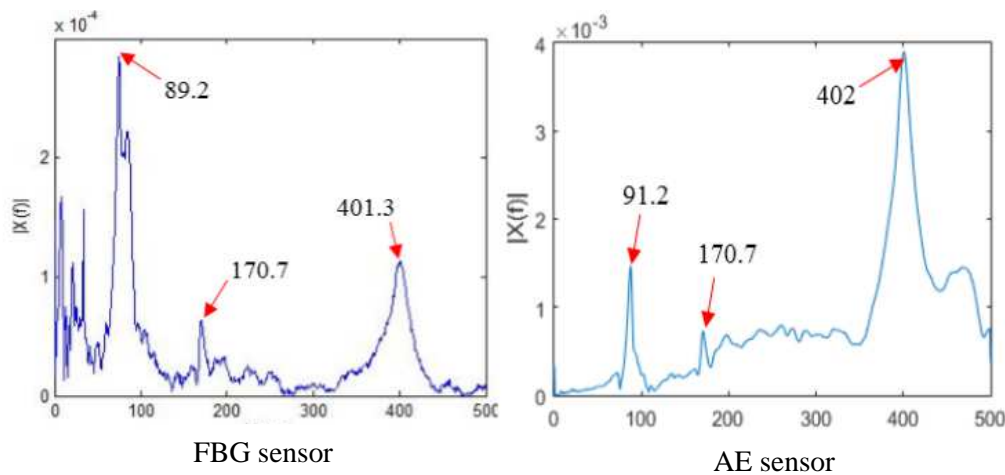FBG sensor   AE sensor

Figure 11. Comparison of natural frequency between FBG and AE sensor
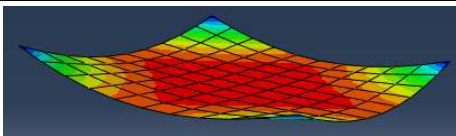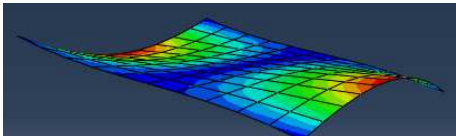
Table 4. Summary of natural frequency results
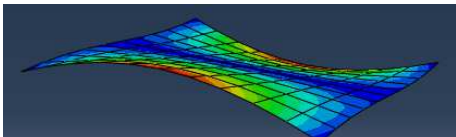
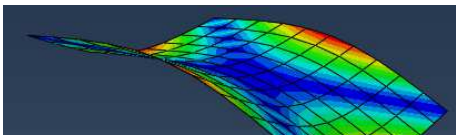| Mode	Natural frequency (Hz)							
	FBG				**AE**			
	Trial 1	**Trial 2**	**Trial 3**	**Average**	**Trial 1**	**Trial 2**	**Trial 3**	**Average**
1	90.8	89.1	89.2	89.7	88.7	90	91.2	89.87
2 &3	172.7	172.7	170.7	172	198.7	172	170.7	180.47
4	404	400.7	401.3	402	401.3	398.7	402	400.7

On the other hand, the signals acquired by FBG sensor and AE sensor have revealed a very good agreement. Both sensors able to pick up all modes predicted by FEA, in which the highest percentage of natural frequency variations between both the sensors are only 4.69% for twisting mode wave propagation and 0.32% for flexural wave propagation. However, for FBG sensor, several spectra can be seen at the lower frequency (below mode 1), which is not consistent with any natural frequency content either from ABAQUS simulation or AE sensor. These unwanted spectra are simply recognized

as noise signal response due to utility or power line frequency. Proper filtering can be done to screen out the undesirable signals.

Meanwhile, AE sensor shows a smoother signal compare to FBG sensor. AE sensor is a direct type of sensor where the strain signals are directly converted to electrical signal without any use of external components such as photo detector that can result in the formation of noise. However, FBG sensor has shown its superiority in term of the ability to be embedded in composite structures. All in all, from the dynamic impact results, a remark can be drawn that the embedded FBG sensor has a great potential in replacing the conventional AE sensor for SHM in aircraft composite wings.

Table 5. Summarization of dynamic impact test results

Mode	ABAQUS Mode Shape	Average natural frequency (Hz)			
		Abaqus	FBG	AE	Error (%)
1		99.5	89.7	89.87	0.19
2		181.02	172	180.47	4.69
3		181.02	172	180.47	4.69
4		373.81	402	400.7	0.32

5. Conclusion

The study has successfully presented the application of real-time structural health monitoring system of composite aircraft wing with the embedment of FBG sensor and the use of MATLAB GUI in which the structure is capable of determining the load induced instantly in real-time without any error. The natural frequency obtained from the FBG sensor has significant similarity with AE sensor. All in all, the main objective of this paper to view real-time changes when the structure undergoes several static loadings and dynamic impact is achieved.

References
[1]   Kahandawa G C, Epaarachchi J A, Wang H, Followell D and Birt P 2013 *Sensors and Actuators A: Physical* **194** 1-7
[2]   Kahandawa G C, Epaarachchi J, Wang H and Lau K T 2012 *Photonic Sensors* **2** 203-14

[3]   Di Sante R 2015 *Sensors* **15** 18666

[4]   Chandrashekhar M and Ganguli R 2016 *Mechanical Systems and Signal Processing* **75** 75-93

[5]   Liu P F, Liao B B, Jia L Y and Peng X Q 2016 *Composite Structures* **149** 408-22

[6]   de Moura M F S F and Gonçalves J P M 2004 *Composites Science and Technology* **64** 1021-7

[7]   Anderson E H and Sater J M 2007 *The 14th International Symposium on: Smart Structures and Materials & Nondestructive Evaluation and Health Monitoring* pp 652702--13

[8]   Gilewski W and Al Sabouni-Zawadzka A 2015 *Archives of Civil and Mechanical Engineering* **15** 469-78

[9]   Guo H, Xiao G, Mrad N and Yao J 2011 *Sensors* **11** 3687

[10] Panopoulou A, Loutas T, Roulias D, Fransen S and Kostopoulos V 2011 *Acta Astronautica* **69** 445-57

[11] Mckenzie I and Karafolas N 2005 *Fiber Optic Sensing in Space Structures: The Experience of the European Space Agency*

[12] Lamberti A, Chiesura G, Luyckx G, Degrieck J, Kaufmann M and Vanlanduit S 2015 *Sensors* **15** 27174

[13] Pereira G, Frias C, Faria H, Frazão O and Marques A T 2013 *Polymer Testing* **32** 99-105

[14] Ling H-y, Lau K-t, Cheng L and Jin W 2006 *Measurement* **39** 328-34

[15] Dai Y, Li P, Liu Y, Asundi A and Leng J 2014 *Optics and Lasers in Engineering* **59** 19-24

[16] Zou H, Liang D and Zeng J 2012 *Optics and Lasers in Engineering* **50** 199-203

[17] Hafizi Z M, Epaarachchi J and Lau K T 2015 *Measurement* **61** 51-7

[18] Yang N 2011 *The Journal of Military Electronics & Computing*

[19] Instruments N 2016 *FBG Optical Sensing: A New Alternative for Challenging Strain Measurements*

[20] Zohari M H, Yusof M F, Siregar J P and Sing L K 2015 *J. Electrical Systems "Special issue AMPE2015"*

[21] Zohari M H B 2014 The Applications of Near Infra-Red Fibre Bragg Grating Sensors for Wave Propagation Based Structural Health Monitoring of Thin Laminated Composite Plates. In: *Faculty of Health, Engineering and Sciences*: University of Southern Queensland) p 183

[22] Tsuda H 2006 *Composites Science and Technology* **66** 676-83

[23] Esposito L, Pucillo G P, Penta F and Rosiello V 2016 *Procedia Structural Integrity* **2** 1870-7